Council on Tall Buildings and Urban Habitat Korea

International Journal of
High-Rise Buildings
www.ctbuh-korea.org/ijhrb/index.php

International Journal of High-Rise Buildings
December 2024, Vol 13, No 4, 317-331
https://doi.org/10.21022/IJHRB.2024.13.4.317

Structural Design of China Merchants Bank Headquarters Tower: Part 1 – Systems and Design

Xiaonian Duan[1†], Yueqi Hou[1] and Mingchen Liu[1]

[1]*Structural Engineering Group, Foster + Partners, London, United Kingdom*

Abstract Rising to a height of 388 m with a high slenderness of 9.2 and a side core plan layout, the China Merchants Bank Headquarters Tower in Shenzhen, a typhoon and moderate seismic region, poses major challenges to structural design of both its gravity and lateral force-resisting systems. Tuned Liquid Dampers (TLDs) are adopted to mitigate wind-induced motions for occupant comfort. Energy dissipating outrigger trusses with Buckling-Restrained Braces (BRBs) as diagonal web members are introduced to increase its lateral stiffness and to enhance its energy dissipation capacity in order to improve its seismic performance when subjected to Maximum Considered Earthquake (MCE) shaking. Both TLDs and energy dissipating outrigger trusses with BRBs are first successful applications in tall and supertall buildings in Shenzhen. A substructure analysis method based on the load paths and the capacity design principle is proposed and successfully applied to the analysis and design of the chord members and connections of the outrigger trusses to core walls and perimeter columns.

Keywords Tall Buildings, Tuned Liquid Dampers, Side Core, Outrigger Design

†Corresponding author:
Xiaonian Duan
Tel. +44-20-7943-6547
E-mail:
xduan@fosterandpartners.com

1. Introduction

Located at the southern end of the Shenzhen Bay Super-Headquarters Base, China Merchants Bank Headquarters campus comprises a 388 m tall Headquarters Tower (hereafter referred to as the HQ Tower) with 77 office floors, two office towers of 94 m tall, two office/culture/5-star service apartment towers of 80 m tall, and two podium buildings of which one is a conference centre and the other is commercial. In April 2024, the side core of the HQ Tower tops out and its perimeter moment-resisting frame reaches Level 65 as shown in the site photo in Figure 1(a). Below ground, the integrated deep basement has 5 floors providing spaces for retail, food and beverage, leisure, plant rooms and car parking. The Foster + Partners integrated architectural, structural and building services engineering design team won an international competition for the design of this campus and have subsequently been commissioned by the owner to complete design work of all three disciplines from concept, through scheme to completion of the detail design stage based on current Chinese national and Shenzhen Municipality regulations and design standards, including passing the Guangdong Province Structural Expert Panel Review. A structural 3D BIM model of the overall project is illustrated in Figure 1(b).

The structural height of the HQ Tower to its roof slab



Figure 1(a). Site photo of China Merchants Bank Headquarters campus in April 2024 (Courtesy of Chao Zhang).

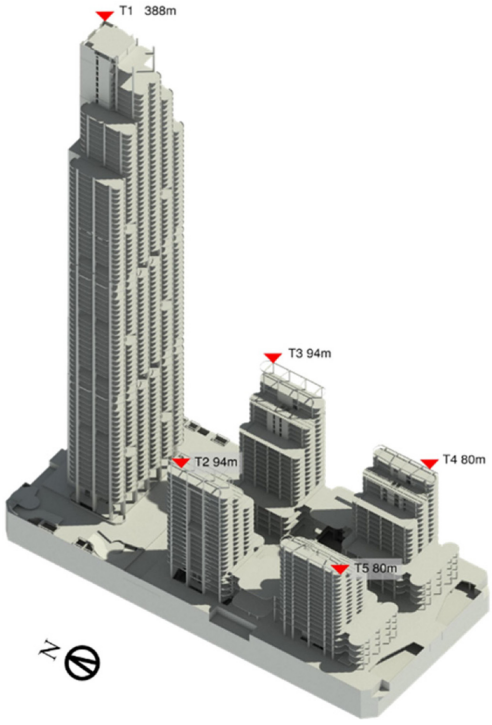


Figure 1(b). Structural 3D BIM model.

level is 387.15 m. The footprint plan dimensions are 68.3 m along the east-west direction and 42 m along the north-south direction, respectively. The ratio between the structural height to the footprint depth along the north-south direction is 9.2, being one of the highest among the many supertall buildings in Shenzhen.

Architectural characteristics of the HQ Tower are: (1) a side core plan as opposed to the conventional central core plan as shown in the typical structural floor framing plan in Figure 2, (2) two levels of setbacks on the elevation, and (3) 20 m long-span column-free large open plan office floor space in the area between the core walls and the perimeter columns on the south façade. When completed, the HQ Tower becomes one of the world's tallest buildings with a side core.

Shenzhen Bay is located in a typhoon region. The 10-minute mean wind speeds at 10 m above ground in an open terrain are 27 m/sec and 35 m/sec corresponding to mean recurrence intervals (MRIs) of 10-years and 50-years, respectively. The site is within a moderate seismic region. For serviceability evaluation to Service-Level Earthquake (SLE) shaking having an average return period of 50 years, the 5% damped short period and 1 second period SLE spectral accelerations are 0.08g and 0.05 g, respectively. For collapse prevention evaluation to Maximum Considered Earthquake (MCE) shaking having an average return period between 2,000 to 3,000 years, the 5% damped short period and 1 second period MCE spectral accelerations are 0.5 g and 0.27 g, respectively. The 50-year MRI wind speed is used for determining the strength design level wind loads together with a wind pressure importance factor of 1.1 and a wind load factor of 1.4.

2. Major Challenges to Structural Design

The HQ Tower poses several challenges to its structural design due to its height of 388 m and a high slenderness ratio of 9.2, as well as its side core architectural plan and two levels of setbacks in its massing. The major challenges include:

- Control of wind-induced drifts and motions as well as torsional irregularity to meet serviceability and occupant comfort criteria and to avoid extreme torsional irregularity.
- Global sidesway buckling stability and limiting second-order effects.
- Height, horizontal and vertical structural irregularities exceed limitations set out in Chinese standards for seismic design of tall buildings. A performance-based seismic design methodology must be adopted, and the structural design must pass a vigorous and rigorous expert panel review process for approval by the Building Official.
- Design of outrigger trusses and their connections to core walls and perimeter columns due to their substantially longer spans of 20 m compared with those in conventional central core tall buildings.
- Design of the floor framing system with spans in excess of 20 m to achieve satisfactory floor vibration performance as well as to facilitate integration of services without increasing the overall depth of the combined structural and service zone.

3. Structural Systems

3.1. The Lateral Force-Resisting System

The lateral force-resisting system of the HQ Tower, as depicted in Figures 3, comprises a reinforced concrete side core, a perimeter moment-resisting frame made of concrete-filled steel tubular (CFT) columns and steel perimeter beams, steel outrigger trusses, belt trusses, and transfer trusses. These outrigger and belt trusses are located at designated refuge floors on levels 32, 43, and 53, where five outrigger trusses on each floor connect the side core walls in the north-south direction to CFT columns on the south façade. With a span of approximately 20 m, these outrigger trusses are significantly longer than those found in conventional central core tall buildings. The belt trusses, also located at refuge floors, connect the perimeter frame to the internal shear walls of the side core in the east-west direction. Figure 4 illustrates the structural framing of a typical refuge floor with the integration of outrigger and belt trusses. In an effort to enhance energy dissipation capability of the seismic force-resisting system along the north-south direction when subjected to MCE shaking, the outrigger trusses are designed to act as energy-dissipating elements, utilizing

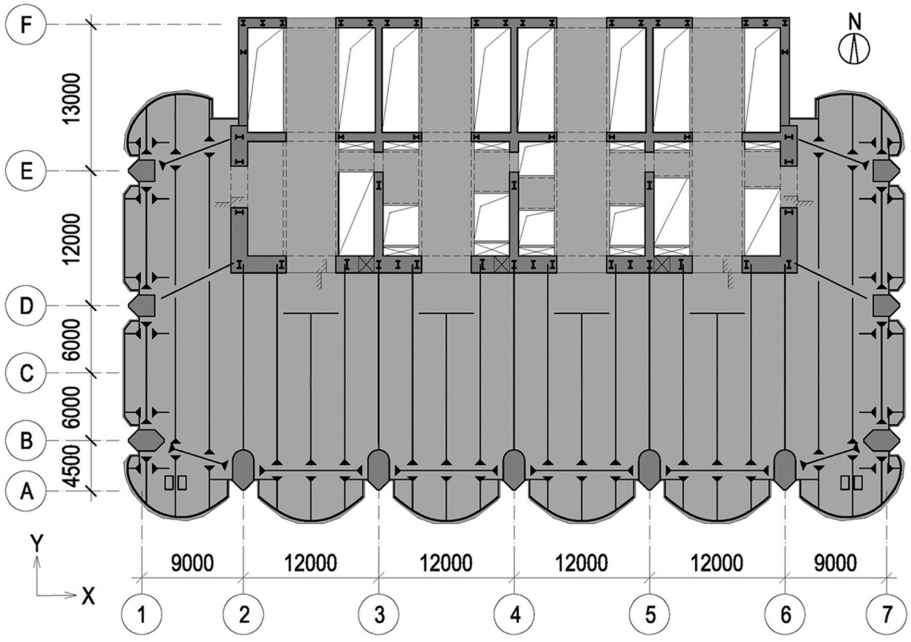


Figure 2. Typical floor structural framing plan.

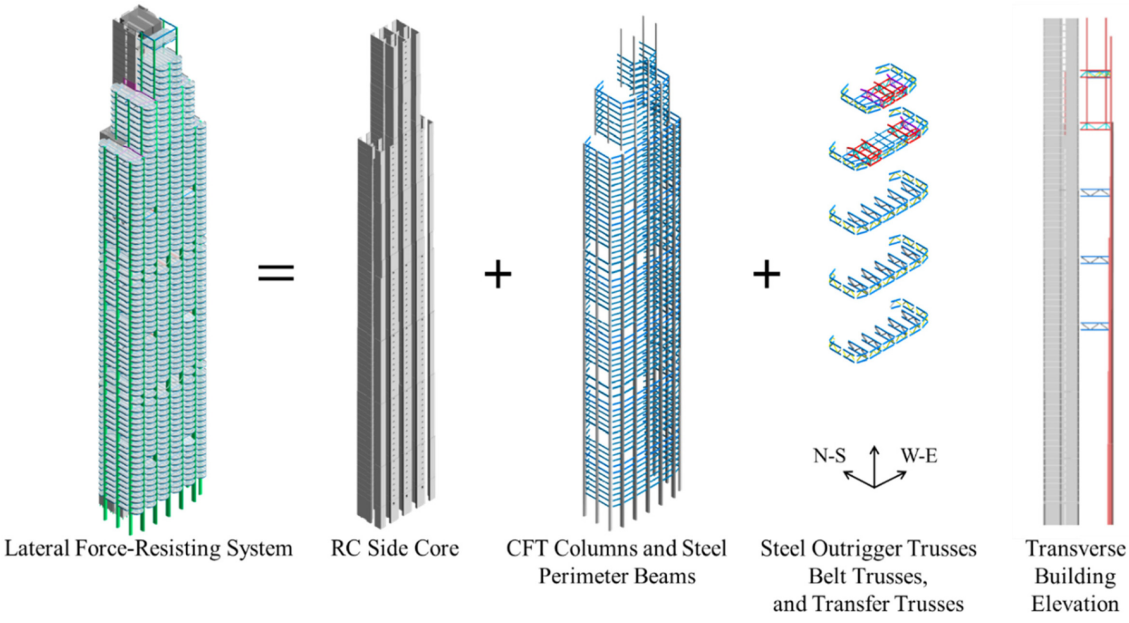


Figure 3. Lateral force-resisting system.

BRBs as their diagonal web members.

Each web member of the outrigger trusses on levels 32 and 43 consists of two BRBs in parallel to withstand both earthquake and wind loads. The strongest BRB has a specified yield strength of 15.5 MN, while the weakest has a specified yield strength of 12.5 MN. The yield strength is determined based on the axial force demands under both the factored SLE and the factored strength design level wind loads as well as full-scale testing capacities currently available in China. Each of the two setback levels 63 and 71 has two outrigger trusses functioning also as transfer trusses supporting discontinued columns above. Since the transfer trusses are classified as critical force-controlled elements, yielding of their diagonal members are not permitted. As a result, all outrigger trusses at these two levels including those not functioning as transfer trusses are designed as conventional steel outrigger trusses as depicted in Figure 5.

3.2. The Floor Gravity Force-Resisting System

The office floor gravity force-resisting system, located outside of the side core, consists of composite cellular

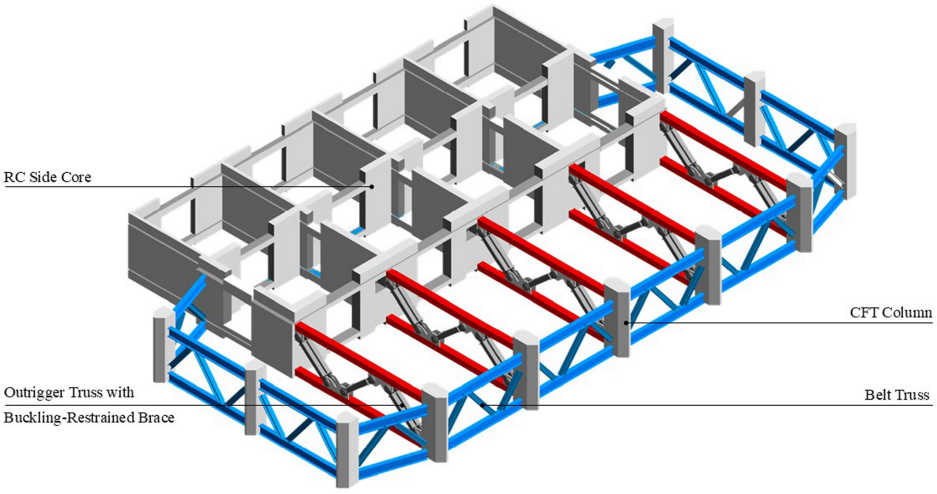


Figure 4. Structural framing of a typical refuge floor with integration of outrigger and belt trusses.

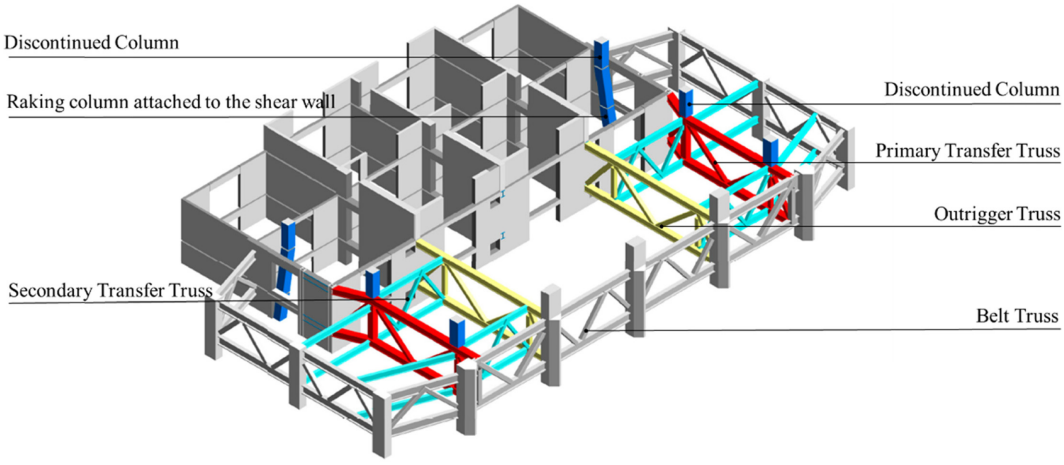


Figure 5. Structural framing of the lower setback level (Level 63) integrating transfer trusses, outrigger trusses and belt trusses.

beams with cast-in-place reinforced concrete floor slabs. Flat steel-bar truss metal decks, rather than profiled steel floor decks, are adopted, reducing typical office floor slab thickness to 120 mm. The composite cellular beams have a depth of 900 mm and span up to 20 m, providing column-free large open office spaces. The composite cellular beams generally span along the north-south direction, supported by shear walls at the north end and perimeter moment frame beams or columns at the south end. In order to integrate the junction of air service ducts adjacent to the coupling beam of the side core for supply air, return air and exhaust air within the floor structural zone, those composite cellular beams which would otherwise have clashed with the ducts are transferred by non-cellular beams to adjacent cellular beams, as shown in Figure 6(a). This framing arrangement also avoids the high shear forces in the coupling beams, which are energy dissipating elements when subjected to MCE shaking, arising from connecting these heavy long-span floor beams directly onto the coupling beam. Between the perimeter columns, the floor features cantilevered curved bay-windows that showcase the south elevation of the HQ Tower. Within the side core, the floor is made of cast-in-place reinforced concrete slabs.

The notched ends of 550 mm depth of the composite cellular beams allow for passage of major service ducts, while branch ducts run through the openings in the webs. Spatial coordination of the integrated multidiscipline design, including service distributions and architectural lighting and ceiling boards, is carried out using BIM tools, as presented in Figure 6(b), to achieve the clear ceiling height required by the owner.

3.3. The Foundation System

The site geotechnical investigation reveals that completely weathered and slightly weathered granite appear approximately 24 m and 42.5 m below the natural ground surface, respectively, with medium-soft and medium-stiff soil layers above the former and strongly and moderately weathered granite sandwiched in between. Based on

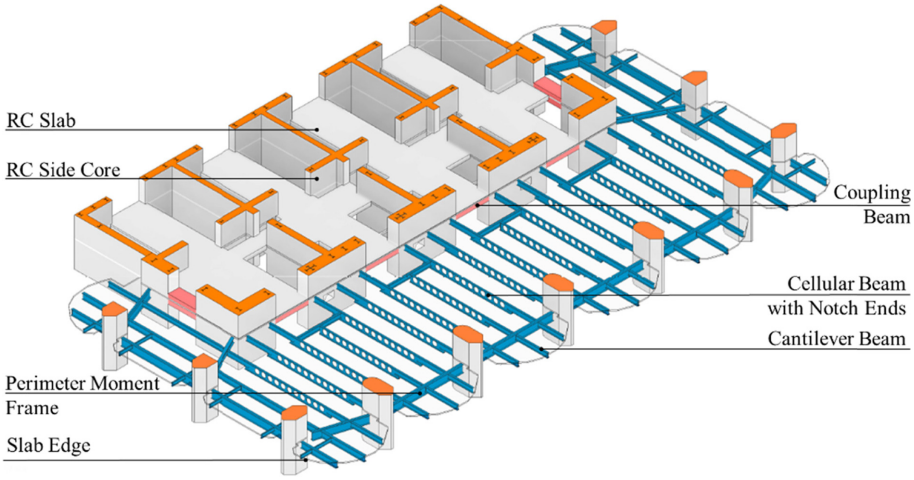


Figure 6(a). Typical floor framing system (floor edge beams not shown).

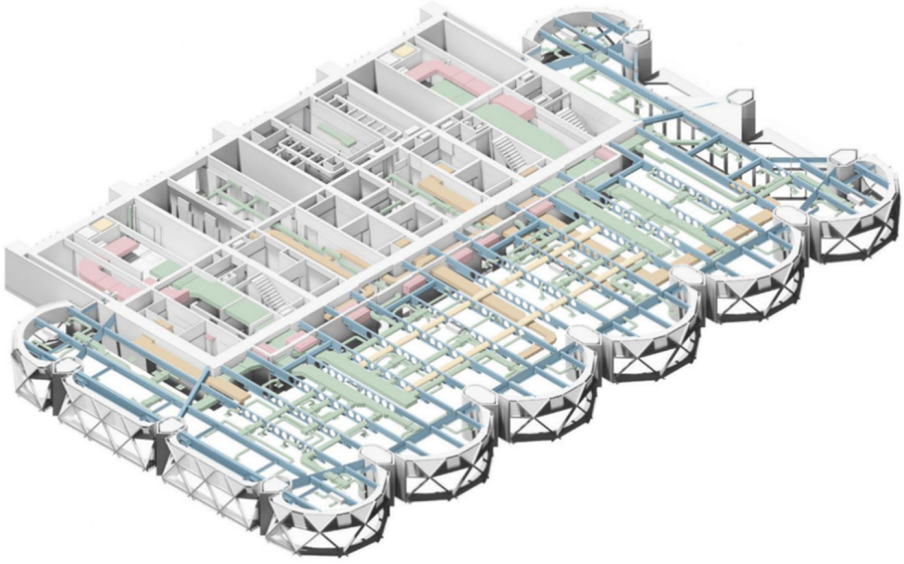


Figure 6(b). Typical floor BIM model Integrating architectural, structural and MEP elements.

recommendations in the geotechnical engineering report, A raft foundation founded on bored cast-in-place end-bearing piles is selected as the foundation system supporting the cores and columns of the HQ Tower, with the slightly weathered granite as the load-bearing layer. Contribution of skin friction from other layers to the load-bearing capacity of the piles is neglected. Piles have diameters of 3.0 m and 2.8 m, respectively, and are arranged in groups below and near the core walls and the perimeter columns. The thickness of the raft slab is 3.7 m and 3.5 m in the regions of the side core and the perimeter columns, respectively.

4. Application of TLDs to Reduce Wind-Induced Motions

4.1. Wind Tunnel Testing Results

The owner commissioned the wind tunnel laboratory of China Academy of Building Research to perform wind tunnel testing of the HQ Tower model to determine floor-by-floor wind loads induced by windstorms of 1-year, 10-year, and 50-year MRIs and to evaluate the motions at the top occupied floor, with and without supplementary damping, induced by windstorms of 1-year and 10-year MRIs, respectively. The scope of work of the wind tunnel laboratory also includes estimation of the available supplementary damping which TLDs are capable of providing together with verification scaled-model testing.

Results obtained by the wind tunnel laboratory based on wind tunnel model testing and structural dynamics computations indicate that, without supplementary damping, the peak resultant accelerations at the top occupied floor induced by the across-wind effects of the windstorms of 10-year and 1-year MRIs is 0.274 m/s^2 and 0.22 m/s^2, respectively, exceeding the occupant comfort criteria of

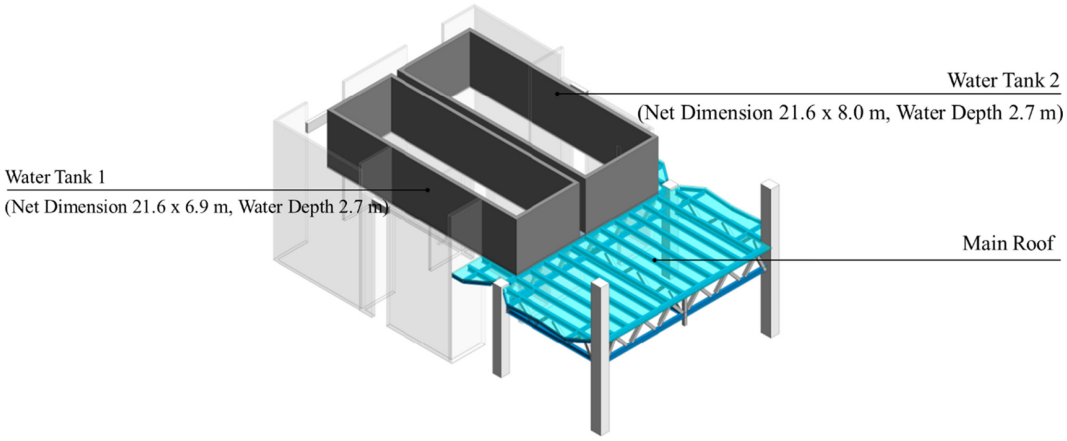


Figure 7. RTLDs (water tanks) and main roof.

0.25 m/s^2 and 0.14 m/s^2 set out in the Chinese design code for tall buildings (MHURD, 2010) for the 10-year MRI windstorm and in ISO 10137-2007 (ISO, 2007) for the 1-year MRI windstorm, respectively. The inherent damping ratios are conservatively assumed to be 1.5% of critical under the 10-year MRI windstorm and 1.0% of critical under the 1-year MRI event, respectively. These results indicate that supplementary damping is needed in order to reduce the wind-induced motions to meet Chinese and international criteria for occupant comfort.

4.2. Selection of the TLD Solution

The top occupied floor of the HQ Tower is a banquet hall located on the 77th floor at the building's summit. Due to space constraints caused by the two setbacks at levels 63 and 71, respectively, floor spaces at and near the top occupied floor are at a premium. In order to locate the supplementary damper on top of the roof slab and still below the 388 m height limit specified in the planning guidelines, a Rectangular TLD (RTLD) solution is employed instead of a Tuned Mass Damper (TMD) solution or a Tuned Liquid Column Damper (TLCD) solution. The TMD solution requires an indoor plantroom of multiple floor high below the roof slab, while the TLCD solution requires a space above the roof slab of several floor high. Both the latter solutions do not meet the architectural and planning constraints. The two independently functioning fire water tanks on top of the roof slab required by Chinese fire codes for tall buildings are proportioned and designed as RTLDs by adding one or more damping screens, thereby freeing up premium floor spaces at and near the top occupied floor in addition to achieving dual-functions of the fire water tanks for a minimal additional cost of adding one or more damping screens. Figure 7 presents the required water depth and the plan dimensions of the two RTLDs positioned on the roof slab.

4.3. Preliminary Design of RTLDs

The length and depth of water of RTLDs can be estimated to match the frequencies of the fundamental natural modes of vibration of the RTLDs and of the HQ Tower along the north-south direction. The frequency of the 1st sloshing mode of water inside a rectangular tank can be determined by the following well-known equation (Lamb, 1932):

$$f_1 = \frac{1}{2\pi}\sqrt{\frac{\pi g}{L}\tanh\frac{\pi h}{L}} \tag{1}$$

Each tank measures L = 21.6 m in length, with a water depth of h = 2.7 m and widths of b = 6.9 m and 8.0 m, respectively. To meet the requirements of the China fire code, the total water volume in the two tanks must reach a minimum of 870 m^3. Tuning of the RTLDs is accomplished by adjusting the tank length and water depth while taking into account the roof geometry and boundary limitations. The widths of the tanks are determined on the basis of the required total volume of water.

The proposed 21.6 m length and 2.7 m depth of water inside the RTLDs result in the frequency of the 1st sloshing mode being 0.12 Hz, matching the fundamental modal frequency of the HQ Tower. Two mechanisms contribute to the damping of the RTLDs, which is the damping of the damper itself rather than the supplemental damping added by the damper to the building. The first is energy dissipation due to viscosity in the boundary layer of water at the bottom of the tanks and the damping ratio of this mechanism can be estimated by the following equation (Tait, 2008):

$$\xi_w = \frac{1}{2\pi}\sqrt{\frac{\nu}{4\pi f_1}}\left(1+\frac{2h}{b}+SC\right) \tag{2}$$

where n is kinematic viscosity of water, which is 1.0×10^{-6} m^2/s. SC is the surface contamination factor assumed to be 1.0. Therefore, the damping of the RTLDs due to kinematic viscosity in the boundary layer of water is approximately

0.04% of critical. The second mechanism is energy dissipation due to damping screens which can increase damping of the RTLDs very significantly. For practical applications the damping due to liquid viscosity is often insignificant compared with the damping resulting from the damping screens (Tait, et al., 2004; Tait, 2008). Results of the project-specific study on wind-induced motions and RTLDs carried out by the wind tunnel testing laboratory (CABR, 2021) indicate that the addition of one damping screen with a 50% solidity ratio and located midway along the length of the tanks significantly enhances the energy dissipation capacity of the RTLDs and is capable of adding a supplemental damping of at least 0.6% and 1% of critical to the HQ Tower when subjected to windstorms of 1-year and 10-year MRIs, respectively.

In addition to tuning of the frequency of the 1st sloshing mode by adjusting the water depth and length as well as enhancing the energy dissipation capacity by installing damping screens in the tanks, another parameter that affects the effectiveness of the RTLDs is the mass ratio between the water mass contributing to the 1st sloshing mode and the generalized modal mass of the building in the fundamental vibration mode. The mass of water contained in tanks can be separated into two parts: (1) impulsive mass (m_0) which is rigidly connected to the tank and moves in-phase with the motion of the building, and (2) mass of the 1st sloshing mode (m_1) which moves out-of-phase with the motion of the building. The inertial force associated with the latter only, rather than the total water mass, counteracts the motion of the building. The value of m_1 can be calculated using the equation below (Graham and Rodriguez, 1952):

$$m_1 = \frac{8}{\pi^3}\rho b L^2 \tanh\frac{\pi h}{L} \tag{3}$$

Therefore, the total mass participating in the 1st sloshing mode of the RTLDs is approximately 77% of the total fluid mass in the two water tanks. The ratio between the total mass of water and the generalized modal mass is approximately 1.1% and that between m_1 and the generalized modal mass is approximately 0.85%.

4.4. Effectiveness of RTLDs

Based on wind tunnel testing results and numerical computation of structural dynamics and shallow wave fluid dynamics, the predicted wind-induced motions (CABR, 2021) at the top occupied floor of the HQ Tower with RTLDs installed on the roof are significantly reduced to 0.21 m/s^2 and 0.12 m/s^2 when subjected to windstorms of 10-year MRI and 1-year MRI, respectively, below their corresponding Chinese and international limits for occupant comfort mentioned previously. The benefit of RTLDs in reducing both wind and earthquake loads for evaluation of storey drifts and for strength design is conservatively neglected. In the latter case, results of linear response history analysis performed by the wind tunnel laboratory (CABR, 2021) show that RTLDs reduce earthquake-induced response only very marginally.

5. Control of Second-Order Effects, Wind-Induced Drifts and Torsional Irregularity

The high slenderness ratio of 9.2 poses a challenge to control of second-order effects and wind-induced drifts. Part of the design solution is to introduce outrigger trusses at refuge floors to enhance the lateral stiffness. Part of the structural analysis solution is to account for all known unfavourable factors affecting the lateral stiffness in order to achieve more accurate estimates of second order effects and wind-induced drifts. Design solutions for avoiding extreme torsional irregularity are maximizing the torsional stiffness of the side core and increasing the lateral stiffness of the perimeter moment frame by introducing belt trusses, as discussed in the following sections.

5.1. Unfavourable Factors Affecting Lateral Stiffness

5.1.1. In-plane flexibility of floor slabs

It is commonly assumed that floor slabs have an infinite in-plane stiffness. However, this assumption can lead to an underestimate of the axial deformation of the chord members of outrigger trusses, particularly in cases where the spans of outrigger trusses are longer than those in conventional tall buildings with central cores. The finite in-plane stiffness of the floor slabs should be taken into account when evaluating storey drifts and second order effects, in order not to overestimate the lateral stiffness. To account for the reduced stiffness resulting from cracking of floor slabs, a 50% reduction in in-plane stiffness is conservatively applied at levels of outrigger truss chords.

5.1.2. Deformation of the basement

Deformation of structural elements in deep basements may significantly increase the sidesway of the above

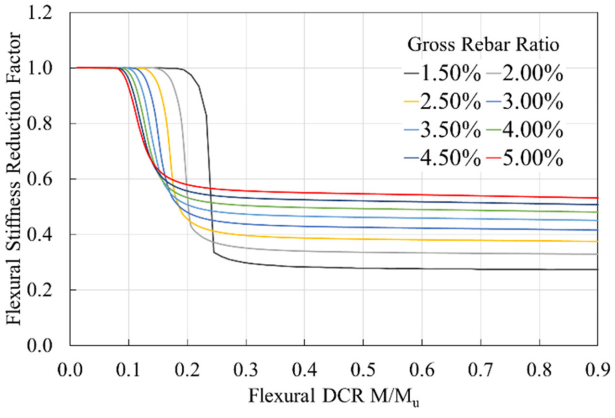


Figure 8. Typical flexural stiffness reduction factors for coupling Beams.

ground towers. One mitigation measure is to extend core walls of the superstructure to form fin walls between the core and the perimeter columns in the basement. However, in the case of the HQ Tower, the large open spaces on the basement floors between the side core and the CFT columns perform critical functions of drop off and lift access, making this mitigation measure impractical. Therefore, it is necessary to consider the deformation of the basement by explicitly modelling the basement structural elements in the global structural analysis model and assuming the basement perimeter walls be laterally restrained by the surrounding soil.

5.1.3. Cracked stiffness of reinforced concrete elements

When evaluating wind-induced drifts and motions, it is important to adopt the reduced stiffness of reinforced concrete members due to cracking. The coupling beams are particularly susceptible to cracking under both wind loads and seismic excitations. Therefore, their cracked stiffness requires careful evaluation. ACI 318-19 (ACI, 2019) recommends a flexural stiffness reduction factor of 0.5, which is approximately equal to 1.4 times the stiffness reduction factor 0.35 for elastic analysis at the factored load level, for coupling beams under service-level wind loads. However, more accurate estimates can be obtained through moment-curvature analysis based on reinforcement quantity provided. Figure 8 shows typical relationships between the longitudinal reinforcement ratio, flexural moment demand capacity ratio (DCR), and the flexural stiffness reduction factor for coupling beams in the HQ Tower obtained by moment-curvature analysis. Results shown in Figure 8 tend to suggest that the flexural stiffness reduction factor for reinforced concrete coupling beams ranges from 0.3 to 0.6, with greater longitudinal reinforcement ratios resulting in lower reductions in flexural stiffness.

Reduction of flexural stiffness of shear walls and CFT columns are not considered under service-level wind loads, as in this case tensile stresses are not present in the former and flexural demands are low on the latter. This assumption is consistent with recommendations of using 1.4 times the flexural stiffness reduction factor of 0.7 for walls and columns for elastic analysis at the factored load level in ACI 318 – 19 (ACI, 2019).

5.1.4. Second-order effects

P-Δ effects reduce the lateral stiffness and result in increased drifts, storey shears and overturning moments. These are considered in the global structural analysis of the HQ Tower subjected to lateral loads.

5.2. Wind-Induced Drifts and Sidesway Displacements

In typhoon regions such as Shenzhen, control of wind-induced drifts is one of the primary objectives in structural design of tall and supertall buildings. The wind loads with a MRI of 50 years, rather than SLE shaking, governs the required lateral stiffness for serviceability.

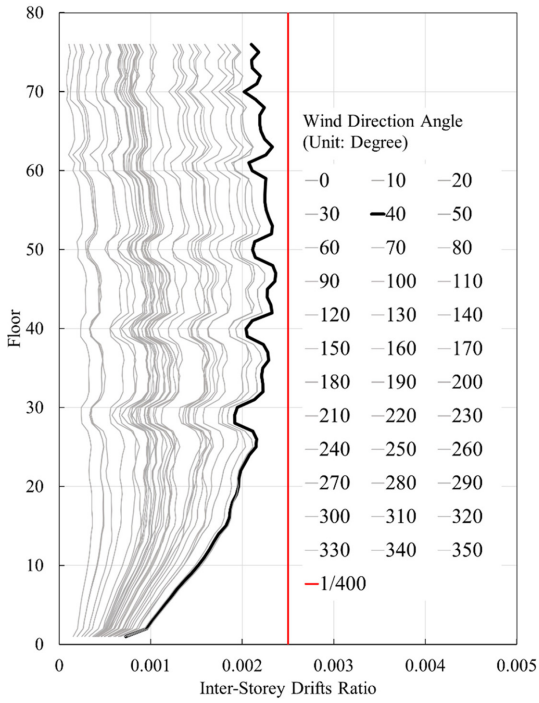


Figure 9(a). Inter-storey drifts ratio in the north-south direction.

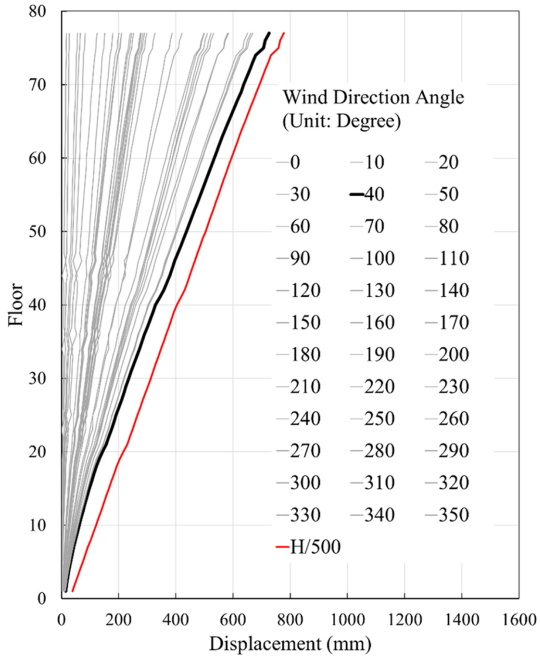


Figure 9(b). Floor sidesway displacements in the north-south direction.

The storey drifts and the sidesway displacements induced by floor-by-floor wind loads determined by wind tunnel testing along 36 wind directions with a MRI of 50 years are presented in Figure 9. The maximum storey drift ratio of 1/423 and the maximum roof sidesway displacement of H/536 are within the acceptance limits of

1/400 and H/500 discussed and agreed with the Guangdong Province Structural Expert Review Panel.

5.3. Control of Second-Order Effects and Global Sidesway Stability Analysis

Control of second-order effects is by means of achieving an elastic critical buckling load of at least 9 times the factored gravity loads for the lowest global sidesway buckling mode. This is the approach recommended in the local Shenzhen Standard SJG 98-2021 (HCBSZ, 2021) for effective control of second-order effects of tall and supertall buildings. In addition to this local standard, reference is also made to the European Union standard Eurocode 3 Part 1-1: General rules and rules for buildings (CEN, 2005). In accordance with this EU standard, second-order effects may be neglected if this multiple is equal to 10 or greater.

Moreover, the method of assessing and limiting the stability coefficient (q) as recommended in Section 12.8.7 of ASCE 7–16 (ASCE, 2017) is also adopted. According to this US standard, if the value of the stability coefficient θ is equal or lower than 0.1, second-order effects are not required to be considered.

After meeting the limits on wind-induced drifts, stability analysis of the HQ Tower is carried out following both the local and international standards considering all the known unfavourable factors described earlier. The computed elastic critical buckling load of the 1st global sidesway buckling mode is 9.1 times the factored gravity loads and the computed stability coefficient θ is 0.09. These results suggest that second-order effects in the HQ Tower is not significant and may even be neglected according to the US standard. Nevertheless, second-order effects are considered in all lateral load analysis of the HQ Tower.

5.4. Control of Torsional Irregularity

Due to its side core plan layout, there exists a significant eccentricity between the centres of mass and the centres of rigidity of the HQ Tower when lateral forces act along the east-west direction, although the structure is symmetric about the north-south axis passing through the centres of mass. In order to avoid extreme torsional irregularity while accepting torsional irregularity, two design measures are implemented. Firstly, the distribution of core wall thickness is optimized to increase the torsional stiffness and to shift the centres of rigidity of the side core towards the centres of mass as much as practical. Secondly, five belt trusses are introduced at the same levels of the outrigger trusses to increase the lateral stiffness of the perimeter moment frame at the south façade. The adopted acceptance criteria require that both the maximum storey drifts and the maximum floor sidesway displacements at one end of the structure of all floors, computed including a 5% accidental eccentricity, should remain within 1.4 times but are permitted to

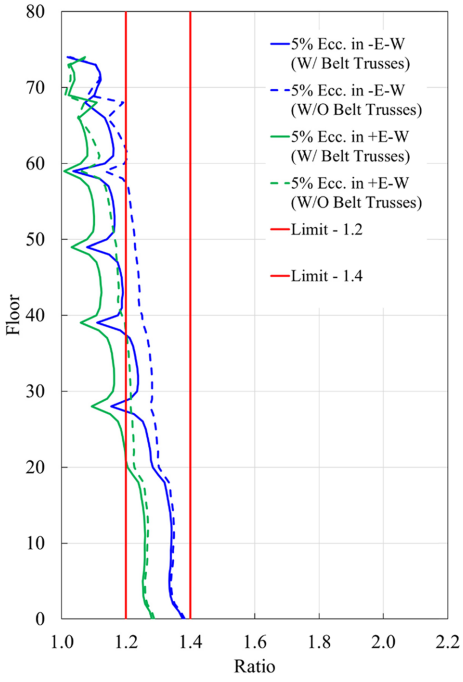


Figure 10(a). Torsional inter-storey drifts ratios in the east-west direction.

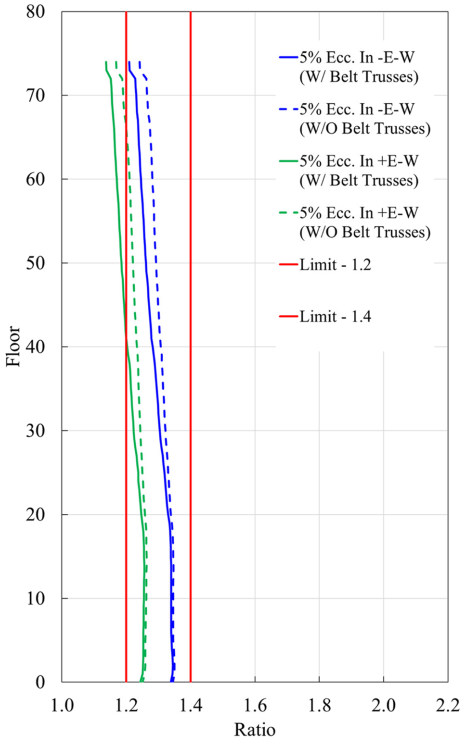


Figure 10(b). Torsional floor displacement ratios in east-west direction.

exceed 1.2 times the average storey drifts and floor sidesway displacements. Figure 10 shows the ratios between the maximum storey drifts and the maximum floor sidesway displacements at one end and the average drifts and the average floor sidesway displacements, together with the

Table 1. Modal participating mass ratios

Mode	Modal Period (sec)	U_x (E-W)	U_y (N-S)	R_z (Torsion)
1	8.44	0.0%	64.9%	0.0%
2	8.13	65.6%	0.0%	4.4%
3	4.85	2.2%	0.0%	68.8%

corresponding limits of 1.2 and 1.4 for torsional irregularity and extreme torsional irregularity, respectively. Figure 10 also demonstrates the significant contribution from belt trusses to reduction of the degree of torsional irregularity.

Table 1 below presents the modal participating mass ratios of the first three natural modes of vibration. It can be observed that lateral-torsional coupling between translation along both the Y (N-S) and the X (E-W) directions and torsion is minimized and insignificant.

6. Design of Outrigger Trusses and Their Connections

The energy dissipating outrigger trusses with BRBs as web members acting as structural fuses not only enhance the energy dissipation capacity of the global structure but also limit the forces developed in the chord members and connections along the two load paths – truss-to-core wall and truss-to-CFT column when subjected to MCE shaking. Both the chords and the connections along the two load paths are critical force-controlled components and must be designed based on the capacity design principle in order to ensure yielding occurs in the BRBs only. However, the global nonlinear response history analysis model may cause "leaking" of forces out of the two load paths and significantly underestimate forces developed along them due to the in-plan stiffness of the floor diaphragms connected to the chords in the global analysis model. Since the connection between the steel chords and the concrete floor slabs by headed stud shear connectors is not reliable when subjected to MCE shaking, this load path should be neglected in the design of the chords, the structural steel members embedded in the core walls and the connections along the two load paths. For this purpose, a substructure analysis method is proposed and successfully applied to the analysis and design of the members and connections along the two load paths, including the steel members embedded in the core walls, as described in the following sections.

6.1. Load Path-Based Substructure Analysis Method

The proposed substructure analysis model including simplified boundary conditions is illustrated in Figure 11. The model includes all steel members and connections only along the truss-to-core wall and the truss-to-CFT column load paths. Additionally, adjacent steel floor beams above and below the outrigger truss being analysed are also included. Concrete floor slabs and the concrete

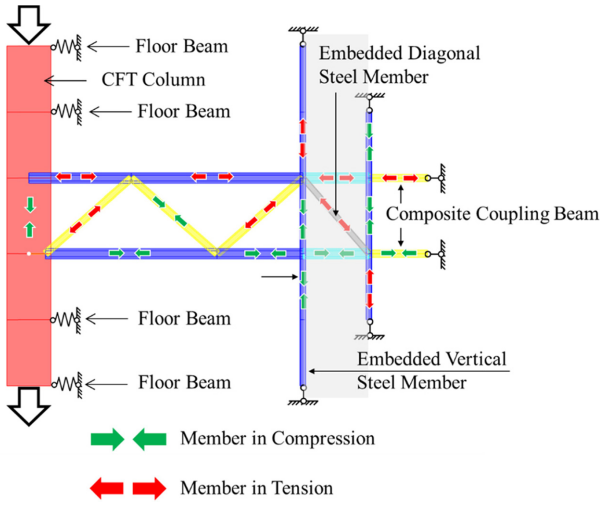


Figure 11. Load path-based substructure analysis model of an outrigger truss.

components in the core walls and the composite coupling beams are excluded in order to prevent "leaking" of forces along the two load paths. The nonlinear static pushover analysis method is employed to evaluate force demands of the force-controlled members and connections along the two load paths. Assumptions on boundary conditions are as follows:

- The vertical steel members embedded in core walls are vertically restrained two levels above and below the chord members of the outrigger trusses.
- The CFT column is assumed to be horizontally restrained by springs with axial stiffness of the steel floor beams at two levels above and below the chord members of the outrigger trusses.
- The steel components of the composite coupling beams are assumed to be restrained horizontally by the core walls at the far ends of the coupling beams.

Nonlinear static pushover analysis is performed by applying upward and downward stepwise increasing displacement loading on the CFT column until all BRB web members are loaded well beyond yielding. The same constitutive model of the BRBs as that adopted in the global nonlinear response history analysis is employed herein. This model takes into account both strain hardening and compression strength adjustment. The pushover analysis stops when the total axial force in one web compression member consisting of two parallel BRBs reaches approximately 40 MN, which is the product of the combined yielding force of 31 MN of the two parallel BRBs with the strain hardening coefficient of 1.2 and the compression strength adjustment coefficient of 1.1. Figure 12 presents the axial force diagram of a substructure analysis model of an outrigger truss on Level 32 at the end of a downward pushover analysis. All force-controlled steel members, components, joints and connections in Figure 12 are designed based on the more unfavourable force demands determined by the separate upward and the

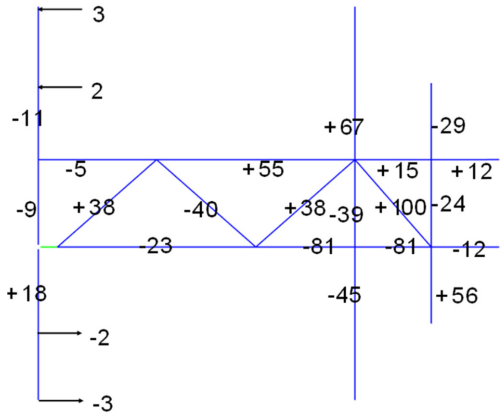


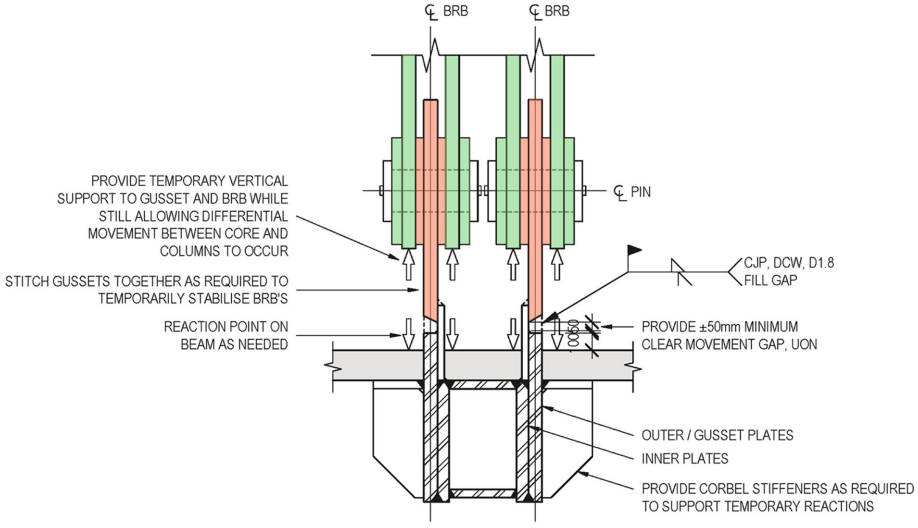
Figure 12. Axial force diagram of a substructure analysis model (+ implies tension and - implies compression, unit MN).

downward pushover analyses. In addition, such pushover analyses also quantify rotational demands of the BRB connections as ranging between 0.029 to 0.034 radians. These large BRB connection rotational demands are accommodated by the pin connection design which provides a large rotation capacity.

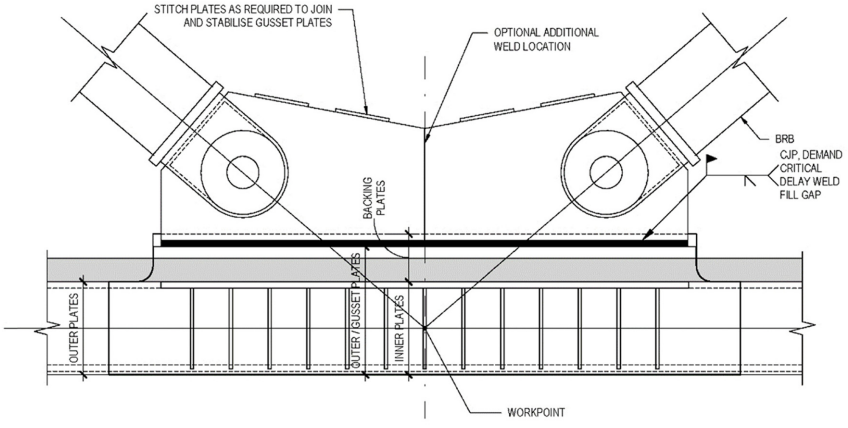
6.2. Design of Outrigger Truss Connections

The parallel BRB configuration of the web members in the outrigger trusses allows for full-scale or near full-scale testing of a single BRB specimen. This setup takes into account the maximum testing capacity currently available in China, as well as the adjusted tensile and compressive strengths of the strongest BRBs specified for the HQ Tower's outrigger trusses. Pin joints are adopted for connections between the BRBs and the outrigger truss frames due to their large rotational deformation capacity.

The chords of the outrigger trusses consist of built-up rectangular hollow sections with two 150 mm thick web plates and two 80 mm thick flange plates. The web plates, made up of 70 mm and 80 mm thick plates, are joined together using a combination of partial-joint-penetration groove welds and additional plug welds for increased integrity. The two 80 mm thick web plates are aligned with and welded to the two gusset plates of the parallel



(a) Section



(b) Elevation

Figure 13. Delayed-welded connection detail at a BRBs-bottom chord joint.

BRBs by delayed demand critical site CJP welds. The delayed CJP welds and a 50 mm clear movement gap between the gusset plates and the 80 mm thick outer web plates are intended to release locked-in forces in the outrigger trusses and to accommodate differential shortening between the core walls and the CFT columns due to differential elastic shortening, creep and shrinkage. A typical connection detail between diagonal web members and a bottom chord is depicted in Figure 13. Fin plates welded to the sides of the web plates of the bottom chords provide temporary support to the BRBs during installation.

Similarly, the connections between the parallel BRBs and the CFT columns are designed as delayed-welded pinned connections with the gusset plates connected to the CFT columns and to the bottom chords by delayed demand critical site CJP welds as shown in Figure 14.

The BRBs and the top chords are connected to core walls by welded connections without delay as illustrated in Figure 15. The 700 mm wide chords are connected to the steel members embedded in core walls through high-performance cast steel nodes. The use of cast steel nodes is necessary because of the limited width of 500 mm only available within the 800 mm thick core walls after allowing 150 mm each side for headed stud shear connectors and reinforcement bars. The high-performance cast steel nodes provide strong connections in the outrigger truss-to-core wall load path and reliably transfer forces to the steel member embedded in the core walls without yielding at the nodal zones.

Figures 16 and 17 show site photos taken during

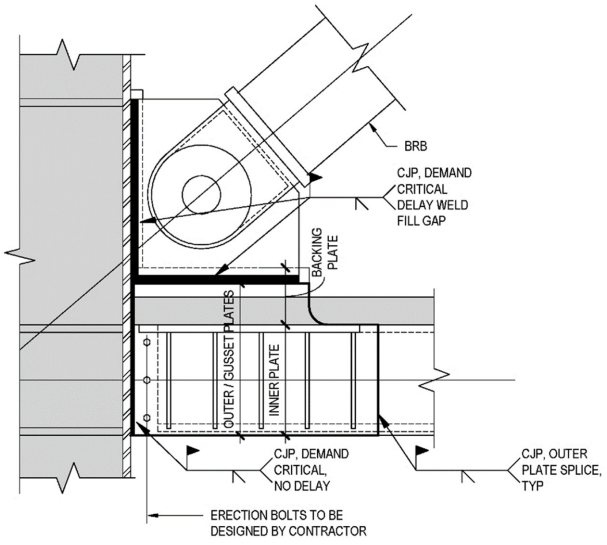


Figure 14. Delayed-welded connection detail at a BRB-CFT Column-bottom chord joint.

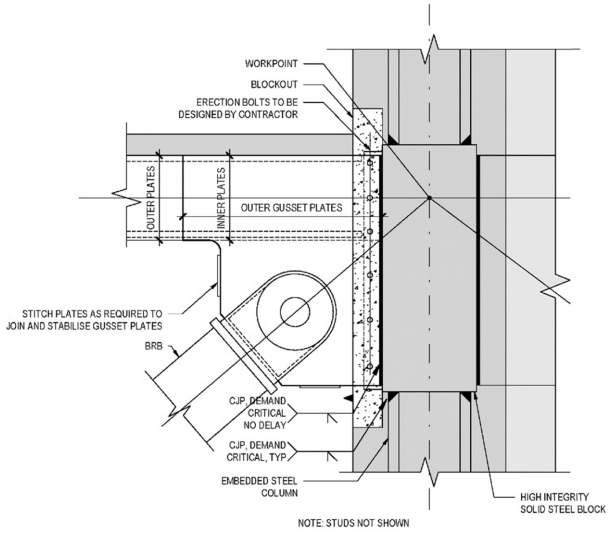


Figure 15. No delay welded connection detail at a BRB-top chord-core wall joint.

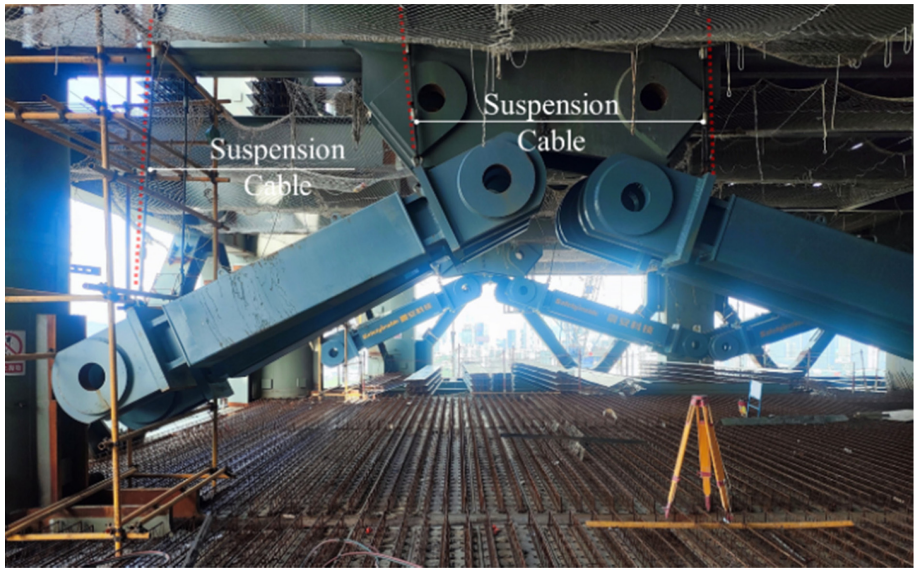


Figure 16. Temporary suspension of the BRBs during erection from the top chord of an outrigger Truss.



Figure 17(a). Site photo of outrigger trusses after installation of BRBs.



Figure 17(b). Site photo of a BRB-to-core wall joint.



Figure 17(c). Site photo of a BRB-top chord joint.

erection and after completion of installation of the BRBs. Temporary suspension of the BRBs by cables from the top chords of the outrigger trusses and lifting into position take place prior to insertion of pins through the gusset plates.

7. Major Challenges and Solutions During Construction

Construction of the HQ Tower follows the conventional bottom up and floor-by-floor sequence. The core walls are constructed using the self-climbing jump-form system which enables fast construction of the side core approximately 15 floors ahead of the CFT columns and floor structures. Except the longer construction cycles of floors connected to the outrigger trusses, a typical construction cycle is approximately one week per floor.

Due to the side core plan layout, the exterior core walls on the north elevation bear little gravity load, while the CFT columns on the southern elevation and the core wall located near the centre of the floor plate support most of the gravity load. Consequently, the CFT columns and the central core walls shorten more than the exterior walls considerably during construction under the self-weight of the structure. This differential shortening induces leaning of the tower towards the CFT columns at the southern elevation. In addition, time-dependent effects of concrete such as creep and shrinkage further increase differential shortening and deviation from verticality significantly. To partially mitigate the southward inclination, the central walls are designed with a greater thickness than the exterior wall. However, a substantial inclination due to self-weight remains. As a result, construction correction measures are adopted by the structural design team and communicated to the contractor. In addition to surveying and monitoring differential shortening and leaning, and correcting for these effects that have happened below, the contractor not only performs staged construction analysis to predict the final configuration at completion and after occupancy considering the construction sequence, schedule and time-dependent effects of concrete but also implements horizontal pre-cambering during construction continuously. Floor slabs are cast to their target elevation levels and the core walls are constructed with a floor-by-floor pre-camber leaning towards the north beyond the target upright positions, such that when the tower deflects laterally toward the south under its self-weight during construction it moves towards the intended uptight configuration upon completion and after occupancy. The above structural analysis and construction correction measures are generally consistent with those outlined by Matar and Faschan (2017).

Additionally, in order to release the locked-in forces in the outrigger trusses arising from the differential shortening between the core walls and the CFT columns during construction, welding between the gusset plates of the pin connection between the BRBs and the CFT columns and the bottom chords of the outrigger trusses are intentionally delayed until structural completion, as shown in Figures 13 and 14.

8. Conclusions

Modern evolving architecture often poses new challenges to structural design of tall and supertall buildings. China Merchants Bank Headquarters Tower has several unique architectural characteristics – a high slenderness ratio, a highly unconventional side core plan layout and 20 m long-span column-free spaces, creating expansive and open office floors. These challenges require innovative structural engineering solutions in both the gravity force-resisting and the lateral force-resisting systems. The unique bespoke floor gravity force-resisting system conceived for this supertall building employs 20 m long-span composite cellular beams with notched ends to form an integrated structural and building service zone and to minimize its depth. This floor gravity force-resisting system enables a 3 m clear floor height together with a 20 m long-span column free space to be achieved within a usual gross floor height of 4.5 m for typical office floors.

As the first applications among the many tall and supertall buildings in Shenzhen, Tuned Liquid Dampers using fire water tanks on the roof and energy dissipating outrigger trusses with Buckling-Restrained Braces as web members are introduced in the lateral force-resisting system. The former reduces wind-induced motions effectively and efficiently and enables both the Chinese and international criteria for occupant comfort to be achieved at the top occupied floor. Compared with conventional outriggers without an effective energy dissipation mechanism, the latter significantly increases energy dissipation capacity and thereby significantly improves seismic performance of this supertall tower subjected to Maximum Considered Earthquake shaking. In addition, the Buckling-Restrained Braces serve as structural fuses limiting the forces delivered by the outrigger trusses to the core walls and the perimeter columns. In order to prevent "leaking" of forces in the load paths of the outrigger force transfer to core walls and perimeter columns in the global nonlinear response history analysis model, a load path-based substructure analysis method is proposed and successfully applied to the design of outrigger chords, outrigger connections to the core walls and perimeter columns, and the steel members embedded in the core walls. This method is based on the capacity design principle and employs the nonlinear static pushover analysis method to conservatively estimate force demands in the critical force-controlled members and connections along the load paths of the outrigger force transfer. The method outlined in this paper may be applied to seismic analysis and design of energy dissipating outrigger trusses and their connections with configurations other than that shown in this paper.

References

American Concrete Institute (2019). Building code requirements for structural concrete (ACI 318-19), ACI, Farmington Hills, MI.

American Society of Civil Engineers (2017). ASCE standard 7-16 Minimum design loads and associated criteria for buildings and other structures, ASCE, Reston, Virginia.

China Academy of Building Research Technology (2021). China Merchants Bank Global Headquarters Tower-Wind-induced vibration and TLD study report (in Chinese), Beijing, China.

Housing and Construction Bureau of Shenzhen Municipality (2021). SJG 98-2021 Technical specification for concrete structures of tall building, Shenzhen, China.

Lamb, H. (1932). Hydrodynamics, Cambridge University Press, England.

Matar, Sami S., and Faschan, William J. (2017). "A Structural Engineer's Approach to Differential Vertical Shortening in Tall Buildings." International Journal of High-Rise Buildings, Council on Tall Buildings and Urban Habitat, 6(1), 73-82.

Ministry of Housing and Urban-Rural Development (2010). JGJ 3-2010 Technical specification for concrete structures of tall building, Beijing, China.

Tait, M.J., El Damatty, E.A., and Isyumov, N. (2004). "Testing of Tuned Liquid Damper with Screen and Development of Equivalent TMD Model." Wind and Structures, 7(4), 215-234.

Tait, M.J. (2008) "Modelling and Preliminary Design of a Structure-TLD System." Engineering Structures, 30(10), 2644-2655.